Monte Carlo stochastic-dynamics study of dielectric response and nonergodicity in proton glass

Alexei Sinitski* and V. Hugo Schmidt
Department of Physics, Montana State University, Bozeman, Montana 59717
(Received 22 January 1996)

Dynamics of the O-H$\cdots$O bond proton glass of the type $M_{1-x}(NW_4)_xW_2AO_4$ (M=Rb or K, W=H or D, A=P or As) has been simulated using the Monte Carlo stochastic-dynamics method that allows one to simulate real time dynamics. The simulation is based both on microscopic interactions of protons and on interaction with an external static electric field. The polarization decay and response to step field has been compared with the Kohlrausch-Williams-Watts stretched exponential form and with predictions of a microscopic ''bound charge carrier'' model. Studying the proton dynamics by a field cooling simulation has revealed nonergodic behavior at low temperatures. [S0163-1829(96)07526-1]

I. INTRODUCTION

Proton glass is an Ising pseudospin glass with a random bias field.[1,2] The Ising pseudospins are the O-H$\cdots$O protons which have spin 1 if located on one side of the H bond, and spin -1 if on the other side. These pseudospins (called spins from here on) interact with each other and with a random bias field originating in the random cation placement. This random bias field smears out the dielectric permittivity cusp one would otherwise see, in analogy with the magnetic susceptibility cusp[3] seen in magnetic spin glasses as temperature decreases.

The prototype proton glass discovered by Courtens[4] is $Rb_{1-x}(NH_4)_xH_2PO_4$ (RADP), a mixed crystal whose parent constituents are RbH_2PO_4 (RDP) which is ferroelectric (FE) below $T_c=147$ K, and $NH_4H_2PO_4$ (ADP) which is antiferroelectric (AFE) below $T_N=148$ K. Both crystals have the same tetragonal structure at room temperature in the paraelectric (PE) phase. Because Rb^+ and NH_4^+ ions are nearly the same size, good crystals over the whole range $0<x<1$ can be grown. The frustrated FE and AFE interactions suppress both the FE and AFE transitions in the range $0.22<x<0.74$. As temperature drops for crystals in this x range, the normal PE behavior goes over into proton glass (PG) behavior, but only gradually because of the random bias field. Accordingly one can speak of PE and PG regimes, but not of distinct PE and PG phases.

Numerous dielectric experiments have been performed on proton glass, spanning the range from audio[5–7] through radio and microwave[8] frequencies and (in the broader sense) into the infrared,[9] and into the Raman[10,11] and Brillouin[12] scattering regimes. Except for the highest frequencies (Brillouin and above) at which one sees inertial effects associated with local and phonon mode effects, these experiments disclose a relaxational response resulting from stochastic jumps of protons within their hydrogen bonds. Specifically, the dielectric ac response of proton glass starts at high temperatures in the PE phase as a soft mode similar to that of the FE crystal[9] and moves on cooling to lower frequencies, transforming into a structural relaxation mode in the PG regime. As is characteristic of disordered systems, this mode has a frequency spectrum significantly wider than that of Debye relaxation, which indicates emergence of a large spread of permittivity time constants with decreasing temperature.

The physical processes governing the dynamics on the microscopic scale are the transverse optical mode, the acoustic shear mode, and the proton relaxation mode. In the optical mode, the phosphate and alkali (or ammonium) ions, which alternate in chains lying along the c axis, oscillate against each other. In the shear mode, the unit cell distorts away from its tetragonal cross section due to motion in the ab plane. In the relaxational mode, the protons make stochastic yet correlated jumps within their hydrogen bonds by a process unique to hydrogen-bonded crystals. This process consists of three parts. First, ''Takagi groups'' or ''bound charge carriers'' are created by the process

$$H_2PO_4+H_2PO_4\rightarrow HPO_4+H_3PO_4.$$

Next, these carriers in effect diffuse through the crystal by the processes

$$HPO_4+H_2PO_4\rightarrow H_2PO_4+HPO_4,$$

$$H_3PO_4+H_2PO_4\rightarrow H_2PO_4+H_3PO_4.$$

Finally, the carriers annihilate by the process

$$HPO_4+H_3PO_4\rightarrow H_2PO_4+H_2PO_4.$$

The optical, shear, and relaxational modes interact, but at the lower frequencies (below about 10^{11} Hz) the relaxational mode can be treated as responding to the average positions of the heavy ions involved in the optical and shear modes.

Dielectric measurements have recently been applied to study the nonergodic behavior of polarization in the PG regime. Below some temperature the upper time constant limit becomes infinite or at least longer than the observation time, indicating the onset of nonergodicity. In the nonergodic regime, the system cannot reach a new state of minimum free energy required by changing external conditions (temperature, field, pressure, etc.) The onset of nonergodicity has been studied by Levstik *et al.*[13] and by us[14] using the field cooling technique, in which the polarization is measured in a cycle consisting of successive zero field cooling (ZFC), field heating (FH), field cooling (FC), and zero field heating (ZFH) processes. Below the temperature of the onset of nonergodicity T_c, the value of polarization at given temperature

and electric field depends on whether this state of the crystal has been obtained in a FH or FC process.

Theories for proton glass begin with the Slater/Takagi model for FE crystals of the RDP type[15,16] and the Nagamiya and other theories for AFE crystals such as ADP.[17,18] The coupling of these theories to explain proton glass properties in mixed crystals because of frustrated FE and AFE interactions has been done in several different ways.[19–21] In all of these models, the interactions between the ''acid'' O-H$\cdots$O bond protons (or deuterons) can be represented as Ising interactions between pseudospins. The acid protons also feel a bias in the time average if they have one neighboring NH_4^+ ion which is hydrogen bonded to one of the proton's oxygen neighbors, while the other oxygen has a Rb^+ neighbor which forms no hydrogen bond with it. The bias effect cannot be represented by a pseudospin-pseudospin interaction; in pseudospin language it is represented as a random bias field interacting with the pseudospin. So far, quantum effects have been considered relatively unimportant in proton glass behavior, except insofar as they determine the pseudospin-pseudospin coupling strength which depends strongly (about a factor of 2) on whether the crystal is deuterated.

Previous computer simulations have been made by Selke and Courtens,[22] who used the Monte Carlo Metropolis algorithm to reproduce the topology of the experimentally determined phase diagram, by Grimm and Parlinksi,[23] who studied the local motion of protons in a two-dimensional glass model for deuterated RADP by means of a molecular-dynamics method, and by us[1,24] employing the Monte Carlo stochastic-dynamics approach.

This paper continues with a description in Sec. II of the proton-proton interactions used in this simulation. Section III explains the basic program outline and important details of the algorithms used. The results for the step electric field response (Sec. IV) and for nonergodic behavior (Sec. V) are then described, analyzed, and compared with the experimental data. Finally, we outline in Sec. VI our other Monte Carlo results and what direction future simulations should take.

II. MODEL INTERACTIONS

We now describe the interactions[1,21,25] employed in general in our simulation technique, together with numerical values of these interactions (in units of the Slater[15] temperature $T_{\rm Slater}=\varepsilon_0/k_B$) employed in the simulations reported in this paper. According to the Slater model[15] the ferroelectric transition temperature T_c (in a pure ferroelectric crystal such as RbH_2PO_4) is given by $k_BT_c=\varepsilon_0/\ln 2$, so ε_0 in temperature units ranges from 70 to 160 K for various ferroelectric crystals which are constituents of proton and deuteron glasses.

The specific interactions[1,22] we employ in our simulation are as follows.

(i) Interaction between two protons at the top, or two protons at the bottom, of a PO_4 group.

(ii) Interaction between one proton at the top, and one proton at the bottom, of a PO_4 group; these two interactions together give both the Slater energy ε_0 which is higher for the nonpolar than for the polar W_2AO_4 groups and explains the ferroelectric transition, and the Takagi energy ε_1 which is the creation energy for Takagi[16] WAO_4 and W_3AO_4 groups. The Takagi groups are ''bound charge carriers'' whose effective diffusion by means of proton intrabond transfer in O-H$\cdots$O bonds is the major mechanism for polarization change in these crystals. Our choices for the interaction energies ε_0 and ε_1 yield $\varepsilon_1=5\varepsilon_0$.

(iii) Interaction of two protons across an ammonium ion from each other which reflects the ammonium ion's proclivity to form strong hydrogen bonds only with two oxygens which are adjacent in a projection along the tetragonal axis, out of the four more or less tetrahedrally arranged oxygens which it bonds to. This interaction causes the antiferroelectric transition in the fully ammoniated crystal. In mixed crystals this interaction together with the previous two ''ferroelectric'' interactions constitute the frustrated interactions which lead to proton glass behavior.

(iv) A corresponding interaction, probably weak (zero in this simulation) between the above two hydrogens but in the case that the cation site is occupied by an alkali ion and not ammonium.

(v) A parallel-bond or dipolar interaction (zero in this simulation) between protons which are close to each other but not attached to the same PO_4, so that this interaction is mostly of the electric dipole type; this interaction is satisfied for both the ferroelectric and antiferroelectric observed phases.

(vi) An interaction between the proton and the lattice, which is nonzero only if one of the oxygens in its O-H$\cdots$O bond is H bonded to an ammonium ion, while the other oxygen's cation neighbor is an alkali ion and not ammonium; this is the random bias interaction while all the other interactions (i)–(v) are pseudospin-pseudospin interactions. The positive value 0.4 in this simulation tends to repel the proton away from the oxygen which is hydrogen bonded to an ammonium ion.

(vii) An interaction with a static external electric field applied along the tetragonal axis of the crystal. In the field each proton has additional energy U_e whose sign is determined by the sign of the proton pseudospin.

The disagreement of the theories on which interactions are present or are significant for proton glass behavior, and the fact that these are mean-field theories which take random cation placement into account only in an average way, emphasize the need for Monte Carlo simulations in which the cations can be placed randomly, and any desired number and strength of interactions can be included in the model without greatly increasing simulation run time. In particular, simulations of dynamic phenomena can be made almost as easily as for static effects, while development of theories for dynamic phenomena is rather difficult and various approximations must be made.

III. MONTE CARLO PROGRAM DESCRIPTION

We begin the simulation by specifying run parameters and initial conditions. Run parameters include temperature, electric field, crystal size, interaction energy parameters, run length, interval between storage of output parameters, and fraction x of ammonium ions. The initial conditions available are a completely ferroelectric proton configuration, a completely antiferroelectric one, and a random configuration obtained as the result of a previous run. Output parameters

include internal (configurational) energy, polarization, and the fractional numbers of the two types of ferroelectric H_2PO_4 groups and the four types of antiferroelectric groups.

At the start of each run, each cation is specified to be an NH_4^+ ion if a random number r $(0<r<1)$ is less than x, and a Rb^+ ion if $r>x$. This randomness, together with the randomness of the proton jumps described below, insures that the simulation has essentially the same randomness as the actual crystal.

The body of the calculation consists of moving protons from one end of their O-H$\cdots$O bonds to the other with probabilities based on temperature and on the proton's interactions with other protons, with the lattice, and with any external electric field.

We use the following method to decide when the protons make their intrabond jumps:

$$\text{O-H}\cdots\text{O}\leftrightarrow\text{O}\cdots\text{H-O},$$

which are responsible for the unique features of proton glass dynamics. Starting with the protons in the chosen initial configuration, we calculate the configurational energy change B resulting as each proton jumps to the other side of its bond. This energy is based on the Ising pseudospin interactions of the proton with its neighboring protons, with the lattice, and with the external field, as explained in Sec. II. From this energy change B, the temperature T, and a random number R, we calculate, from Eq. (2) below, the time T_J when each proton will jump. The proton with the earliest jump time T_{J1} is found from this timetable, and is moved to the other end of its bond. The ''clock'' measuring the total elapsed time is advanced to T_{J1}, and energy changes B are calculated for its next jump and the jumps of the neighbors it interacts with. Then new jump time intervals T_J are calculated for this proton and its neighbors, and corresponding jump times $T_{J1}+T_J$ are entered into the timetable. The earliest jump time T_{J2} in the new timetable is found, and the above procedure is repeated. The process is continued until the total number of jumps specified as the run length is reached. This approach, similar to one developed by Bortz, Kalos, and Lebowitz,[26] allows us to perform real-time dynamic simulations.

We use the following procedure to calculate the time interval T_J in attempt time units from one jump of a given proton to its next jump. First, we calculate the resulting configurational energy change B. Then, a random number generator selects a random number R between 0 and 1. This R has the physical significance that the function $R(T_J)$ is the probability that the proton will not jump in an interval T_J since its previous jump. It obeys the differential equation

$$-dR/dt=\nu_0 R/(1+e^{B/T}),$$

which in terms of $T_J\equiv\nu_0 t$ (ν_0 equals jump attempt frequency) becomes

$$-dR/dT_J=R/(1+e^{B/T}).$$

For each R within an interval dR, there corresponds a T_J within an interval dT_J. The correct correspondence between R and T_J is obtained by integration:

$$-\int dR/R=-\ln R=\int dT_J/(1+e^{B/T})=T_J/(1+e^{B/T}); \tag{1}$$

$$T_J=-(1+e^{B/T})\ln R. \tag{2}$$

Here, $1+e^{B/T}$ is the jump time constant (mean value of T_J) in units of the attempt time (inverse attempt frequency). A common choice of the well-known Metropolis algorithm is 1 if B is negative and $e^{B/T}$ if B is positive; this gives the proper ratio $e^{-B/T}$ for upward and downward jump probabilities. Our choice is less common but also obeys the detailed balance condition and does not have an artificial kink in time constant vs B at $B=0$.

The time evolution of crystal parameters is partially preserved by storing, after every I_w jumps, the FE order parameter, the two AFE order parameters, the configurational energy, the clock time in units of the attempt time, and percentages of each type of H_yPO_4 group, where $y=0$ to 4. The final crystal configuration is stored also. The FE order parameter is at the same time a properly normalized polarization P ($P=1$ for a completely polarized crystal). It is this normalized polarization that we discuss hereafter.

A recent modification to the program allows us to switch the static external field on or off after a certain number of jumps. We have performed two types of simulations involving the field. First, we have studied the polarization response to an electric field step. Starting from the ferroelectric configuration, we compare the polarization decay without the field and its rise in the electric field both for FE ($x=0$) and PG ($x=0.5$) crystals. These runs have been performed at various temperatures and values of the electric field. The number of steps in these runs is 2×10^5, and the field is applied in the middle of the run.

A second program modification allows us to study the nonergodic behavior of the proton glasses by modeling the cycle of the ZFC, FH, FC, and ZFH processes. After a run at a given temperature we calculate the average value of the polarization and change the temperature by a small step (the largest $\Delta T=0.01$ in units of the Slater temperature). Since the dynamics of the system at low temperatures is slow, we have to increase the total number of jumps up to 10^7 for each temperature. Consequently, such simulations consume considerable computer time, requiring a few weeks of computation on our HP-Apollo 9000/720 workstation.

IV. RESPONSE TO STEP ELECTRIC FIELD

In the first above-mentioned type of simulation we obtain both the decay from a fully polarized configuration without field and the polarization rise from zero in the external field. We check the results against the exponential law

$$P/P_i=\exp[-(t-t_1)/\tau_1], \tag{3}$$

where P_i is the initial polarization and τ_1 is the time constant. The simulated decay starts only after at least one pair of ''bound charge carriers'' has been created, so we must use an additional parameter t_1 to offset the beginning of decay from $t=0$. To describe the polarization rise in the field to its final value P_f we use the expression

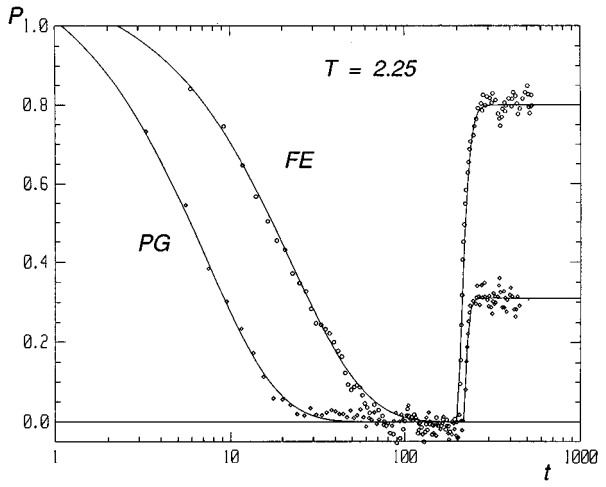

FIG. 1. Normalized polarization as a function of jump time (in attempt time units) for FE (circles) and PG (diamonds) model samples at a high temperature (in units of T_{Slater}). The polarization decays from a fully polarized initial condition (solid lines: Debye relaxation) and rises after applying the external field (solid lines: KWW law).

$$P/P_f = 1 - \exp[-(t-t_2)/\tau_2]. \tag{4}$$

Here the parameter t_2 offsets the start of rise to the moment t_2 when the field is applied.

When the polarization decay becomes ''nonexponential,'' we check it against the phenomenological Kohlrausch-Williams-Watts (KWW) ''stretched exponential'' law, given by

$$P/P_i = \exp[-(t/\tau)^{\beta}], \tag{5}$$

where τ is the ''time constant'' and β is a ''stretch exponent'' between 0 and 1.

The decay is also checked against the expression from our ''bound charge semiconductor'' model, which is rather complicated but which in the proton glass temperature regime has approximately a ''logarithmic gaussian'' form given by

$$P/P_i = \exp[-\ln^2(1+t/\tau)]. \tag{6}$$

We omit the obvious counterparts of expressions (5) and (6) for the case of polarization rise.

We have made simulations for the values of external field energy $U_E = 0.1$, 0.3, and 0.5 (in units of Slater temperature T_{Slater}) both for FE ($x=0$) and PG ($x=0.5$) model crystals. These simulations were made on a ''crystal'' consisting of $8\times8\times8=512$ unit cells (4096 protons) with periodic boundary conditions. We do not recalculate U_E to the exact value of actual external electric field, but a simple estimate shows that fields employed in our simulations are about one order of magnitude higher than those available in practice. We have to choose such high values in order to obtain more pronounced data.

The simulations show the expected result, that the decay takes place with a single time constant at high temperatures and down to the onset of proton glass behavior. Figure 1 shows the typical results for $T=2.25T_{\text{Slater}}$, $U_E=0.5$ for FE and PG samples. Both decays are well described by Debye relaxation (3). The polarization rise for the FE crystal is described by the KWW law (5) with an unusual value of ''stretch exponent'' $\beta=1.25$. We ascribe this fast ''squeezed exponential'' rise of polarization to the extremely high value of external field, since the results for $U_E=0.1$ give $\beta=1$. For the PG sample the polarization rise is stretched even at high temperatures, $\beta=0.9$.

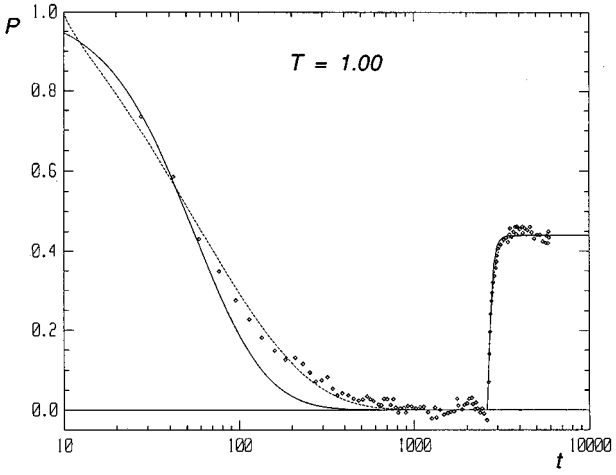

FIG. 2. Normalized polarization as a function of jump time (in attempt time units) for PG model sample at a low temperature. Solid line: ''bound charge carrier'' model; dashed line: KWW law.

As temperature decreases, the FE sample undergoes the ferroelectric phase transition and the number of jumps in our simulations has been too small to observe the extremely slow relaxation, which would be governed by domain wall migration. The PG sample has no phase transition and develops a larger and larger spread in time constants. In the proton-glass state the polarization behavior (shown in Fig. 2 for $T=T_{\text{Slater}}$, $U_E=0.5$) can be satisfactorily described both by the ''stretched exponential'' law (5) and the ''bound charge carrier'' model (6). We see that (6) works better at the initial stage of decay, while (5) takes over at later stages. Though we cannot clearly distinguish the two alternatives using the data obtained so far, the simulation results are in good qualitative agreement with dielectric experiments[5–11] that show nonexponential response in the PG regime. Future simulations are planned to determine more closely the shape of the response, to apply the exact expression for P from the ''bound charge carrier'' model, and to obtain the temperature dependence of the parameters involved.

V. NONERGODIC BEHAVIOR

For studying nonergodic behavior we consider the normalized polarization P as a function of time at each temperature. Typical plots of P vs t are shown in Fig. 3 (note the different time scales for high- and low-temperature curves). At high temperatures P quickly relaxes to equilibrium after the temperature change, so the plot of P vs time is generally horizontal with some fluctuations. Below the ergodic temperature, equilibrium cannot be reached during the time of ''observation,'' and slow relaxation occurs as sudden jumps of P. These jumps, instead of a smooth asymptotic behavior, result from the finite size of the model crystal. The cause of the polarization change is the diffusion of the Takagi pairs.

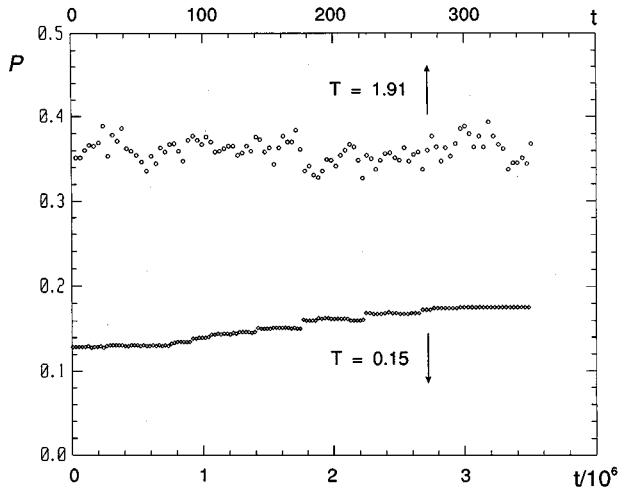

FIG. 3. Typical time dependence of polarization in the field-heating process. Note the different time scales for high (circles, $T=1.91$) and low (diamonds, $T=0.15$) temperatures.

When our small model sample has no Takagi pairs at all, the polarization is frozen in for a long time. Then, following the creation of a pair, the polarization changes. After the annihilation of the pair the polarization is frozen in at a new level.

We take the average value of P as the polarization at a given temperature, because one might consider the computer as a ''measuring device'' that returns the quantity averaged over the observation time. Calculations that specify the total elapsed time (in attempt time units) rather than the total number of jumps for each run will probably better simulate the real experiment, in which temperature is changed by steps at a constant rate. However, this modification of the program will waste computer time for runs at high temperatures, because the system will remain unchanged for a long time after equilibrium has been reached. We have not yet performed such simulations.

The average value of P is plotted against T in Figs. 4 and 5, to display temperature dependence of normalized polarization for each process of cooling and heating. The results of

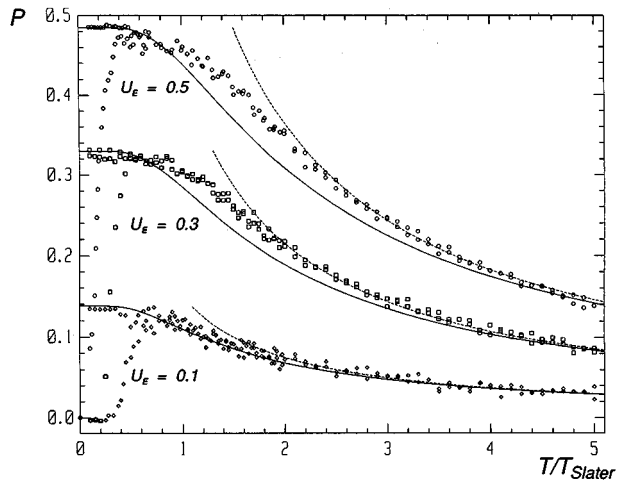

FIG. 4. Field-heating and field-cooling processes for three values of external field.

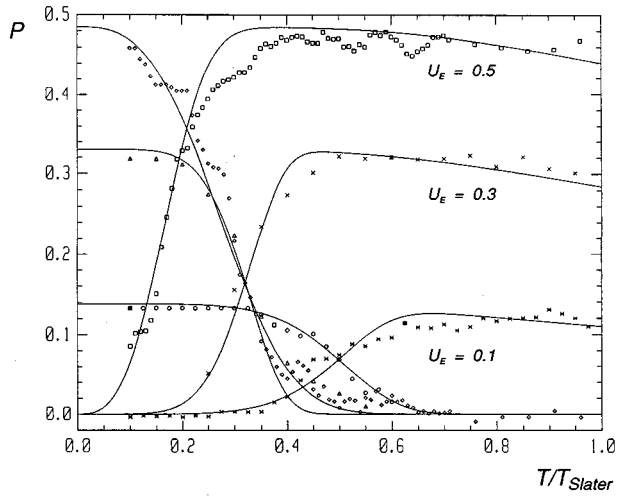

FIG. 5. Field-heating and zero-field-heating processes for three values of external field.

the nonergodic behavior simulations are in good qualitative agreement with the experimental data.[13,14] Figure 4 shows the field heating and field cooling processes for three values of the external field energy U_E. At high temperatures the normalized polarization obeys the Curie law $P=C/T$ (shown by dashed lines) both for FH and FC runs. At lower temperatures we see departure from this law. The FC behavior can be qualitatively described by the formula

$$P=P_i\tanh[C/(P_iT)]. \tag{7}$$

This expression (shown by solid lines) gives the Curie law with the same constant C as the high-temperature expansion and allows for the low-temperature saturation of P. We see that for the lowest field, $U_E=0.1$, Eq. (7) gives a good description in the whole temperature range. For higher fields, however, the description is worse. We attribute this discrepancy to the nonlinear behavior in an electric field much higher than attainable in a real experiment.

Figure 5 shows the low-temperature parts of the FH and ZFH processes. This behavior can be described by the generalization of Eq. (7) in the form

$$P=\{P_i-(P_i-P_f)(1-\exp[-(T/T_e)^\gamma])\}\tanh[C/\{\cdots\}T], \tag{8}$$

where the missing factor in the hyperbolic tangent is the same as in the braces, T_e is the ergodic temperature, and P_i and P_f are the initial and the final values of polarization, respectively.

Equation (8) describes the ZFH process when $P_f=0$. For this process

$$P\cong P_i\exp[-(T/Te)^\gamma], \tag{9}$$

because in the tanh argument $\{\cdots\}T<C$ at low temperature because T is small, and at higher temperature because $\{\cdots\}$ is small.

For the FH process, one first sets $P_i=0$ in Eq. (8) and then sets $P_f=P_i$. Then

$$P\cong P_i(1-\exp[-(T/Te)^\gamma]) \tag{10}$$

TABLE I. Parameters of the fit to the ''bound charge carrier'' model. External field energy U_E, Curie constant C, and ergodic temperature T_e are given in units of the Slater temperature. The exponent γ and the initial and final polarization P_i, P_f are dimensionless. The last column shows the total number of jumps for each temperature in the low temperature regime.

U_E	C	T_e	γ	P_i, P_f	MCS (LT)
0.1	0.15	0.53	6	0.138	0.1×10^6
0.3	0.43	0.37	6	0.33	10×10^6
0.5	0.73	0.19 (FH)	3	0.485	5×10^6
		0.31 (ZH)			

at low temperature because the tanh factor is near unity. At higher temperature, P approaches the expression of Eq. (7).

The parameters used in the fit to Eq. (8) are shown in Table I. The values of the exponent γ are of special interest. The following simple considerations[14] based on the bound charge semiconductor model[27,28] give $\gamma=6$. The dielectric relaxation results from the diffusion of HPO_4 and H_3PO_4 ''bound charge carrier'' groups by means of intrabond proton transfer. Below the ergodic temperature T_e the random potential barriers encountered by these groups are so high that on a reasonable time scale the diffusing groups are confined to some regions. During the observation time the polarization in the inaccessible portion of the crystal remains frozen in. Thus the amount of polarization change must be proportional to the volume of the regions accessible to the diffusion. The diffusion takes place in a fractal potential with individual potential steps distributed randomly up and down.[28] Therefore, the maximum barrier encountered in diffusing N net steps is proportional to $N^{1/2}$ (this is similar to the dependence $r\propto N^{1/2}$ for position vs step number in the well-known ''drunkard's walk''). At a given temperature T, the diffusion distance possible in a reasonable time is thus proportional to T^2, and the volume available to the diffusing group is proportional to T^6. However, more elaborate analysis[29] that takes more details of the bound charge semiconductor model into account but still makes some approximations gives $\gamma=3$. Surprisingly, the T^6 dependence better fits the experimental results.[14,29] Our computer simulations give $\gamma=6$ except for the highest field, when the best fit has been obtained with $\gamma=3$. Thus presently we cannot distinguish the two possibilities from our simulations.

Another puzzle revealed in the simulations is the strong dependence of the ergodic temperature T_e on the electric field. With increasing field one might expect a small decrease in T_e (because the ordering effect of the external field decreases the range of states available to a system), but we did not expect such a strong dependence. Moreover, for the highest field the ergodic temperature differs significantly for the field-heating and zero-field-heating processes. Future simulations are needed to determine whether these results are computer artifacts or are due to the extremely high electric field.

VI. CONCLUSION

The reported results are only the first step in applying the Monte Carlo stochastic dynamics method, but they show that the method is a useful tool for studying the microscopic nature of proton glass. Further simulations and improvements of the algorithm are needed. At low temperatures much of the computer time is spent for the situation when a proton returns to its previous position after the next jump, without changing the polarization of the sample. For better efficiency at low temperatures, the algorithm must directly consider the processes of creation, diffusion, and annihilation of ''bound charge carriers'' rather than the jumps of individual protons. Other possible applications include calculating the ac permittivity in an alternating electric field and applying the method to other proton glass systems, such as the quasi-one-dimensional betaine phosphate–betaine phosphite mixed crystal.[30]

Besides the results reported in this paper, other results have been obtained in the framework of Monte Carlo stochastic dynamics study. The phase diagram including effects of coexistence of the PE/PG phase with the FE or AFE phase has been mapped out. Permittivities for various frequencies have been obtained using Fourier analysis and have been compared with the predictions of our microscopic ''bound charge carrier'' model and with experimental ac permittivity results. Effects of the random bias ''field'' caused by random cation placement have been studied and the paths of the WAO_4 and W_3AO_4 bound charge carriers, which in effect move by intrabond proton transfer, have been followed from creation to annihilation. All these results will be published elsewhere.

ACKNOWLEDGMENTS

Assistance by Paul Schnackenberg, Di He, and Chris Stigers in early stages of this work is gratefully acknowledged. Professor Adolfo Equiluz and Professor George Tuthill of this department helped with questions concerning programming and connection with the San Diego Supercomputer Center. Personnel at this center have given considerable assistance when needed. This work was supported by National Science Foundation Grants No. DMR-8714487 and No. DNR-9017429, in particular with several grants of time at the San Diego Supercomputer Center and with support for undergraduate students. One of us (A.S.) gratefully acknowledges support under the National Research Council CAST (Cooperation Applied Science and Technology) Program.

*Permanent address: Institute of General Physics, 38 Vavilova St., Moscow 117942, Russia.

[1] V. H. Schmidt, Ferroelectrics **72**, 157 (1987).
[2] R. Pirc, B. Tadić, and R. Blinc, Phys. Rev. B **36**, 8607 (1987).
[3] D. Chowdhury, *Spin Glasses and other Frustrated Systems* (Princeton University Press, Princeton, NJ, 1986), pp. 1–35.
[4] E. Courtens, J. Phys. Lett. **43**, L199 (1982).
[5] E. Courtens, Phys. Rev. Lett. **52**, 69 (1984).
[6] S. Iida and H. Terauchi, J. Phys. Soc. Jpn. **52**, 4044 (1983).
[7] Z. Trybuła, V. H. Schmidt, J. E. Drumheller, D. He, and Z. Li, Phys. Rev. B **40**, 5289 (1989).
[8] H. J. Brückner, E. Courtens, and H. G. Unruh, Z. Phys. B **73**, 337 (1988).
[9] J. Petzelt, V. Železny, S. Kamba, A. V. Sinitski, S. P. Lebedev,

A. A. Volkov, G. V. Kozlov, and V. H. Schmidt, J. Phys. Condens. Matter **3**, 2021 (1991).
[10] E. Courtens and H. Vogt, J. Chim. Phys. (Paris) **82**, 317 (1985).
[11] J. L. Martinez, F. Agullo-Rueda, and V. H. Schmidt, Ferroelectrics **76**, 23 (1987).
[12] E. Courtens and R. Vacher, Phys. Rev. B **35**, 7271 (1987).
[13] A. Levstik, C. Filipić, Z. Kutnjak, I. Levstik, R. Pirc, B. Tadić, and R. Blinc, Phys. Rev. Lett. **66**, 2368 (1991).
[14] N. J. Pinto, K. Ravindran, and V. H. Schmidt, Phys. Rev. B **48**, 3090 (1993).
[15] J. C. Slater, J. Chem. Phys. **9**, 16 (1941).
[16] Y. Takagi, J. Phys. Soc. Jpn. **3**, 273 (1948).
[17] T. Nagamiya, Prog. Theor. Phys. **7**, 275 (1952).
[18] Y. Ishibashi, S. Ohya, and Y. Takagi, J. Phys. Soc. Jpn. **33**, 1545 (1972); *ibid.* **37**, 1035 (1974).
[19] P. Prelovšek and R. Blinc, J. Phys. C **15**, L985 (1982).
[20] V. H. Schmidt, J. T. Wang, and P. Schnackenberg, Jpn. J. Appl. Phys. **24**, Suppl. 24-2, 944 (1985).
[21] E. Matsushita and T. Matsubara, Prog. Theor. Phys. **71**, 235 (1984).
[22] W. Selke and E. Courtens, Ferroelectrics Lett. **5**, 173 (1986).
[23] K. Parlinski and H. Grimm, Phys. Rev. B **37**, 1925 (1988).
[24] V. H. Schmidt, Z. Trybuła, D. He, J. E. Drumheller, C. Stigers, Z. Li, and F. Howell, Ferroelectrics **106**, 119 (1990).
[25] V. H. Schmidt, S. Waplak, S. Hutton, and P. Schnackenberg, Phys. Rev. B **30**, 2795 (1984).
[26] A. B. Bortz, M. H. Kalos, and J. L. Lebowitz, J. Comput. Phys. **17**, 10 (1975).
[27] V. H. Schmidt, J. Mol. Struct. **177**, 257 (1988).
[28] V. H. Schmidt, Ferroelectrics **78**, 207 (1988).
[29] V. H. Schmidt and N. J. Pinto, Ferroelectrics **151**, 257 (1994).
[30] S. L. Hutton, I. Fehst, R. Böhmer, M. Braune, B. Mertz, P. Lunkenheimer, and A. Loidl, Phys. Rev. Lett. **66**, 1990 (1991).